An Automatic Braking System That Stabilizes Leukocyte Rolling by an Increase in Selectin Bond Number with Shear

Shuqi Chen and Timothy A. Springer

The Center for Blood Research and Harvard Medical School, Department of Pathology, Boston, Massachusetts 02115

Abstract. Wall shear stress in postcapillary venules varies widely within and between tissues and in response to inflammation and exercise. However, the speed at which leukocytes roll in vivo has been shown to be almost constant within a wide range of wall shear stress, i.e., force on the cell. Similarly, rolling velocities on purified selectins and their ligands in vitro tend to plateau. This may be important to enable rolling leukocytes to be exposed uniformly to activating stimuli on endothelium, independent of local hemodynamic conditions. Wall shear stress increases the rate of dissociation of individual selectin–ligand tether bonds exponentially (1, 4) thereby destabilizing rolling. We find that this is compensated by a shear-dependent increase in the number of bonds per rolling step. We also find an increase in the number of microvillous tethers to the substrate. This explains (a) the lack of firm adhesion through selectins at low shear stress or high ligand density, and (b) the stability of rolling on selectins to wide variation in wall shear stress and ligand density, in contrast to rolling on antibodies (14). Furthermore, our data successfully predict the threshold wall shear stress below which rolling does not occur. This is a special case of the more general regulation by shear of the number of bonds, in which the number of bonds falls below one.

Key words: L-selectin • E-selectin • peripheral node addressin • cell adhesion • microvilli

The initial step in leukocyte accumulation in inflamed tissue is a rolling interaction on the vessel wall. The driving force for rolling is the hydrodynamic force of the bloodstream acting on the adherent cell; rapid formation and breakage of adhesive bonds are required for the adhesive contact between the leukocyte and the vessel wall to be maintained and to be translated along the vessel wall during rolling (4, 27). Rolling occurs in a series of steps or jerks that appear to represent receptor–ligand dissociation events (1, 24, 27, 56). From measurements of the dimension of the adhesive contact zone in the direction of flow and the average step distance, it has been estimated that as few as two adhesive bonds between the cell and the substrate are sufficient to support rolling (1).

The selectin glycoproteins are limited in expression to vascular cells and are specialized to mediate rolling. L-selectin is expressed on leukocytes and binds to carbohydrate ligands on endothelium and other leukocytes; E-selectin and P-selectin are expressed on endothelium and bind carbohydrate ligands on leukocytes. The structures of several of these molecules are known from crystals or electron micrographs (21, 29, 50) and equilibrium constants, kinetics, and effect of applied force on kinetics are known for several of the molecular interactions (1, 4, 31, 32, 50).

Rolling should be an inherently unstable transition state, delicately poised between firm adhesion and lack of adhesion. However, rolling through selectins is highly stable to alterations in selectin density and hydrodynamic force acting on the cell (27); this force is proportional to and can be calculated from the shear stress at the vessel wall. The velocity of rolling cells varies little in vivo or in vitro despite wide variation in wall shear stress (7, 25, 27, 28, 37) (see Fig. 1). This stability in the velocity of rolling leukocytes is likely to be important in the postulated function of rolling as a checkpoint in the process of leukocyte accumulation in inflammation. Rolling enables leukocytes to survey endothelium for signs of inflammation, including chemoattractants that can activate firm adhesion through integrins, and provide directional cues for transendothelial migration (27, 52). Particularly in early or in mild inflammation, leukocytes may roll through a postcapillary venule without developing firm adhesion, and thereby reenter the circulation (6). It appears that a threshold level of activa-

Address correspondence to T. Springer, The Center for Blood Research, Harvard Medical School, Department of Pathology, 200 Longwood Ave., Room 251, Boston, MA 02115. Tel.: (617) 278-3200. Fax: (617) 278-3232. E-mail: springer@sprsgi.med.harvard.edu

tion must be exceeded before firm adhesion is stimulated. Rolling velocity will determine the time duration of exposure of a leukocyte to activating stimuli on the vessel wall, and hence should be of key importance in determining whether activation occurs. Therefore, for proper control of activation of rolling leukocytes, it may be important for rolling velocity to be relatively independent of wall shear stress, which varies widely depending on tissue and physiologic and inflammatory state. Even for different postcapillary venules within a single tissue, wall shear stress can vary markedly; e.g., it ranges from 3–36 dyn/cm^2 for 30–40-μm venules in cat mesentery (23a).

Recently, a number of constants critical to an understanding of rolling at the cellular and molecular level have been measured. Most measurements come from studies of the dissociation rate constants for "transiently tethered" cells. Transient tethers occur when leukocytes in a hydrodynamic flow chamber interact with a substrate, i.e., the lower wall of the flow chamber, that bears selectins or ligands at densities too low to enable rolling (4). Under these conditions, leukocytes moving at the hydrodynamic flow velocity will momentarily bind to the substrate and remain almost motionless, then dissociate and resume movement at the hydrodynamic velocity. Transient tethers have first-order dissociation kinetics and may reflect unimolecular binding and dissociation events. The off-rates extrapolated to no force on the cell (k_{off}°) are 6.6–8.0 s^{-1} for L-selectin, 0.95 s^{-1} for P-selectin, and 0.70 s^{-1} for E-selectin (1, 4, 35). A similar estimate for E-selectin was derived from the jerkiness of rolling on endothelium (24) or on purified E-selectin (56). The faster off-rate of L-selectin is consistent with the similarly faster rolling velocity through L-selectin than E-selectin or P-selectin (37). Although made with a cellular system, the k_{off} measurements with human L-selectin are remarkably similar to those of ≥10 s^{-1} made with a surface plasmon resonance for soluble murine L-selectin binding to a different ligand (32). Experimental studies have also revealed the amount by which force increases k_{off} for selectins, and shown that at least within the range of shear stresses studied, k_{off} increases exponentially with applied force (1, 4, 35) (see Fig. 1). Theory predicts that at higher wall shear stresses, k_{off} will continue to increase (8, 16).

The recent measurements of effect of shear stress on dissociation of tether bonds emphasize our lack of understanding of how rolling through selectins is stabilized. Whereas rolling velocity increases slowly or plateaus with shear (see Fig. 1, open symbols), the rate of transient tether dissociation increases rapidly and exponentially (see Fig. 1, closed symbols). In the absence of any regulatory mechanism to counterbalance the increase by applied force of k_{off}, rolling should be unstable. As shear stress is increased, bonds will break more rapidly and there will be less time for bond formation, so there will be fewer bonds between the cell and the substrate, and more force per bond. The cell should roll faster and faster, and then detach. Similarly, decreasing force should decrease the rate of bond dissociation, allow more time for bond formation, and there should be a tendency for the cell to roll slower and slower until firm adhesion occurs.

This predicted instability has attracted the attention of biophysicists, who have proposed theories to explain rolling. These theories differ widely in their underlying physical models, e.g., the nature of the adhesive contact zone and the rules governing bond dissociation, and were constructed before any measurements of tether dissociation kinetics and effect of applied force were available. All theories assume unstressed off-rates that are 1,000-fold or more slower than those actually measured. Two theories are able to show a plateau in rolling velocity with wall shear stress; however, a very large number of bonds between the cell and the substrate is assumed, which results in smooth rolling instead of jerky rolling as observed (15, 49). Another model is stochastic and gives jerky rolling; however, a plateau in rolling velocity with increasing wall shear stress is not demonstrated (22). Regions of "parameter space" are found that permit rolling; however, this space is quite limited, and a modest decrease or increase in a parameter such as wall shear stress can result in firm adhesion or detachment, respectively (22). Indeed, this is exactly what is observed for rolling on antibodies, although not on selectins (14). Other types of stochastic models do not attempt to construct a physical model, but relate the mean and variance of rolling velocity to kinetics of bond cluster dissociation (56), or use pauses during rolling as a measure of the lifetime of single bonds (24). These are more similar in approach to the work described here, but have not been used to estimate the number of bonds per cluster during rolling, to examine the influence of wall shear stress on the kinetics of bond cluster dissociation, or to compare the kinetics of dissociation of individual bonds to bond clusters.

No current theory on rolling predicts the shear threshold phenomenon, in which no adhesion or rolling is seen through L-selectin below a threshold of ~0.4 dyn/cm^2 wall shear stress (19). This phenomenon is completely unexpected, because as the force on a cell is decreased, better adhesion, not worse adhesion is predicted. However, the shear threshold phenomenon has been confirmed for L-selectin in widely varying experimental conditions (3, 20, 26, 45), and has been extended to E-selectin and P-selectin at lower wall shear stresses (26).

In this paper, we describe a novel control mechanism for stabilizing the state of rolling and the velocity of rolling leukocytes. We measure the kinetics of the discrete steps or "jerks" that occur during rolling, and relate them to the kinetics of transient tethers. Contrary to expectation, we find that as shear increases, the number of selectin–ligand bonds between the cell and substrate increases, and thereby counterpoises the increased off-rate of individual receptor–ligand bonds. Furthermore, we show that during rolling, selectin–ligand bonds are clustered and can resist force collectively rather than individually. Moreover, the number of microvillous tethers between the cell and the substrate increases with shear. An automatic control system is further supported by high regularity in distance and time between jerky steps in certain conditions during rolling, which represent oscillatory rather than stochastic movement. The automatic control system enables leukocytes to reach a dynamic balance between formation and breakage of selectin–ligand bonds over a wide range of wall shear stresses and ligand densities. It explains the stability of rolling, as well as the shear threshold phenomenon.

Materials and Methods

Cells and Substrates

Neutrophils were prepared as previously described (27), and perfused into the flow chamber in Hank's balanced salt solution/10 mM Hepes, pH 7.4 (H/H buffer), with 2 mM Ca^{2+}. A polystyrene Petri dish was coated with an ~5-mm spot of 20 μl of purified peripheral node addressin (PNAd)[1] (36) diluted 1:5, 1:10, 1:20, or 1:40 in TSA (20 mM Tris-HCl, pH 8, 150 mM NaCl, 0.03% NaN_3) with 0.1% of octyl glucoside, or with 20 μl of E-selectin (0.38 or 0.75 μg/ml) in PBS (pH 9) for 1 h at 37°C, followed with 2% HSA for 1 h at 37°C to block nonspecific binding sites. The site densities of E-selectin were determined (14).

Flow Assay

The polystyrene dish was assembled in a parallel plate laminar flow chamber and mounted on the stage of an inverted phase–contrast microscope (Diaphot-TMD; Nikon). For measuring rolling tether duration and rolling velocity, a syringe pump was used to generate the indicated shear stresses (1). To generate a rapid step-wise change in shear stress, a high shear flow was derived by connecting a pressurized air reservoir to the high hydraulic pressure end of the flow chamber with an electronically controlled air valve. A signal synchronized with turning of the valve was recorded on the video tape with the microscopic images of cells for later analysis. Shear stress was calibrated from the flow rate. To estimate the response time of the flow system, the velocity of a freely flowing cell was measured when shear was reduced from 8 to 0.5 dyn/cm^2. The velocity decreased exponentially from the hydrodynamic velocity at the high shear to that at the low shear with a time constant of 0.067 s.

Image Analysis

A computerized imaging system was developed for quantitative cell rolling and tethering analysis. This system consists of a Pentium computer with the MVC 150/40-VL boards (Imaging Technology) and the software developed by us for analysis of rolling adhesion and transient tethering. A TEC-470 charge-coupled device video camera (Optronics) was used. A video frame image consists of 512 × 512 pixels, with a pixel size of 0.89 × 0.73 μm with a 20× objective, and 0.44 × 0.36 μm with a 40× objective. For measuring instantaneous velocity, the center point of a cell was determined from at least 40 top intensity pixels of the cell and the center point was tracked frame to frame, yielding a space resolution of <0.4 μm and <0.2 μm with 20 and 40× objectives, respectively. Two methods were used to define the duration of tethers during rolling, that estimate lower and upper limits of tether duration, respectively. Method 1 could be applied to larger numbers of rolling cells. Images of central areas of cells were segmented by an intensity threshold. Motion analysis was performed by comparing every two successive frames to separate the tethered cells from the cells free in flow. The resultant image of tethered cells was then processed using a convolver with a 4 × 4 square kernel to further detect the central region of each cell with a velocity below a threshold. The threshold was set at ~30 μm/s above the minimum velocity of tethered cells in the flow direction at a particular shear stress, which defined the time period in between step-wise jerky movements. The central regions of the tethered cells were then tracked in real time to determine tether duration. In method 2, tether duration was determined according to the changes in instantaneous rolling velocity in the flow direction above a velocity-valley threshold, which was set from 6 to 36 μm/s corresponding to shear stresses from 1 to 32 dyn/cm^2. Tether duration was defined as the duration from the time when the instantaneous velocity drops >270 μm/s^2 between two or more frames, to the time when the velocity increases >270 μm/s^2 between two or more frames. Tether durations usually began at one velocity peak and extended to the leading edge of the next velocity peak. A rolling cell was selected using a window that included its track across the field of view. The instantaneous velocity of this cell was measured between each frame, and tether duration was determined using the definition described above. Each step distance was determined with the same definition, and the distribution of step distances was derived for individual cells. For measuring rolling velocity, an adjusted intensity threshold and a different kernel for convolution were used to track cells. The imaging system has a time resolution of 0.033 s. The experimental error in measurement of the duration of rolling tethers was dependent on the velocity of the rolling cells, and was +0.033/−0.016 s at 30 μm/s, +0.033/−0.008 s at 60 μm/s, and +0.033/−0.004 s at 120 μm/s. Only the negative component of the error, e.g., −0.004 s at 120 μm/s, affected estimation of k_{off}. The precision of measurement of transient tether and rolling tether duration was high within the scope of this study, i.e., the system error was small when compared with variation in tether duration and k_{off} estimates from experiment to experiment.

1. *Abbreviation used in this paper:* PNAd, peripheral node addressin.

Monte Carlo Simulation

Monte Carlo simulation of the breakage of multiple independent tether bonds was used to estimate the average number of bonds per rolling tether (46). The Bell equation, $\tau = \tau_0 \exp(^{-}F_b \sigma/kT)$, was used to model the lifetime, τ, of a single tether bond as function of force on the bond, F_b; $\tau_0 = 1/k_{off}^{\circ}$. The constants k_{off}° and σ were taken from previous studies on L-selectin and E-selectin (1, 35). In method 1, the lever arm previously measured for transient tethers, 3.06 μm (1), was used to determine the geometry of the tethered cell relative to the substrate, and to relate the hydrodynamic force on the cell to the force on the rolling tether (1, 4). In method 2, the average step distance determined for each individual rolling cell was used as the estimate of the lever arm. The total force was postulated to be equally divided among all bonds remaining at any given time. The initial number of effective bonds, N_b, holding the cell in each step of rolling was assumed to have a Poisson distribution (12). Therefore, simulations were done for varying numbers of initial bonds, and these were added together in the ratios appropriate for a Poisson distribution with different average numbers of initial bonds. To fit to measured kinetics at a given shear stress, a number of simulated rolling tether dissociations similar to that experimentally measured was computed three different times, the χ^2 value for theoretic compared to experimental data were calculated, and the initial number of bonds was adjusted to minimize the χ^2 value. The standard deviations for the three Monte Carlo simulations for each time point of the best fit are shown in figures.

Estimation of Number of Microvillous Tethers

The number of microvillous tethers was determined from the force constants for elongation of individual tethers from neutrophils (41) and the rate of tether elongation during rolling. From the work of Shao et al. (41), the instantaneous force on a single tether f_m has been shown to be $f_m = F_0 + k_2\, dl/dt$. Thus, the average force F_m on the tether in duration T_s of elongation can be estimated as $F_m = F_0 + k_2\,(L_s - L_0)/T_s$, where $F_0 = 45$ pN; $k_2 = 11$ pN*s/μm; L_0, the initial length of a microvillus = 0.35 μm (41), L_s is the stretched tether length, and T_s is the rolling tether duration. Assuming that a total tether force, F_t, is equally distributed over the microvillous tethers, the number of tethered microvilli can be estimated as: $N_m = F_t/F_m$. For each experimental condition of PNAd density and wall shear stress, method 2 was used to determine average step distance and rolling

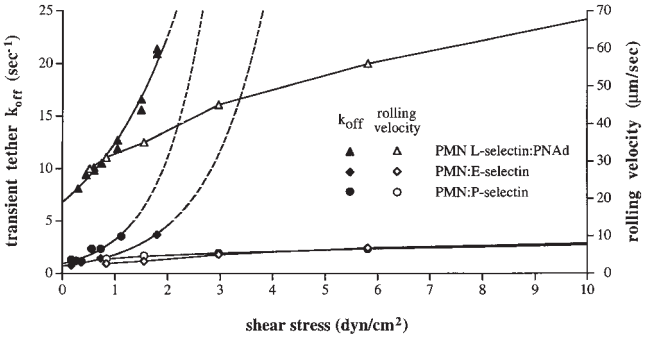

Figure 1. The disparity between effect of shear on rolling velocity and dissociation kinetics of tether bonds. With selectins, leukocyte rolling velocity is highly regulated, i.e., velocity changes little over a wide range of shear, whereas tether bond dissociation kinetics increase exponentially with shear. Rolling velocity data (open symbols) are from refs. 35 and 37. Tether bond dissociation kinetics (k_{off}, closed symbols) are from refs. 1, 4, and 35; regions of exponential curves extrapolated to higher shear are dashed.

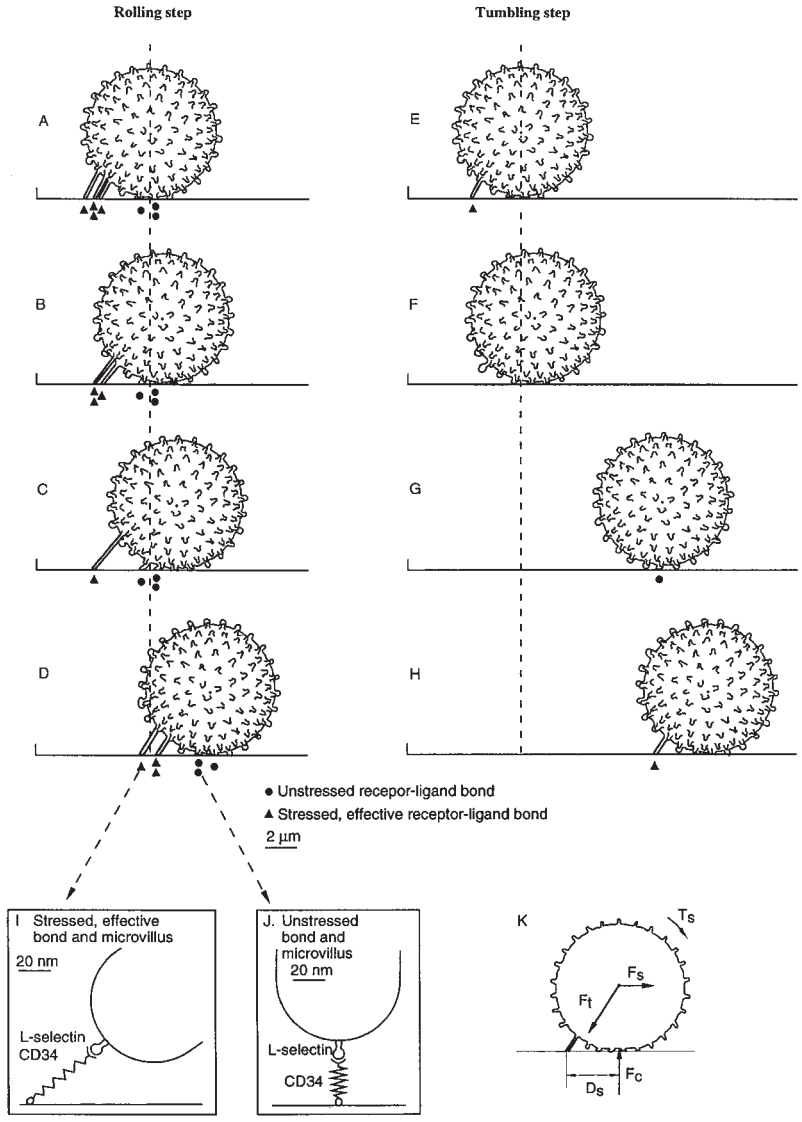

Figure 2. Schematic model of leukocyte rolling through selectins, with dissociation and formation of bonds, and microvillous tether elongation. (A–D) Rolling step. During rolling, the rearmost cluster of tether bonds is subjected to tensile force, and mechanically holds the cell (A). These stressed bonds can be termed the "effective bonds" (I) and are differentiated from unstressed bonds (J). The cell is tethered and moves slowly and smoothly, due to the elongation of microvillous tethers (A–C), while at the same time bonds dissociate (A–D). After dissociation of the last bond, the cell moves step-wise forward in flow (C and D) until it is held by the next cluster of tether bonds (D). (E–H) Tumbling step. A cell is tethered by a certain number of bonds (E). When these tether bonds dissociate, no bond is present (F) and the cell moves a tumbling step downstream until a new bond forms (G) and becomes effective and tethers the cell (H). (K) A cell in hydrodynamic flow is subjected to a hydrodynamic force F_s and a torque T_s generated by shear flow. Because the cell is tethered, it is subjected to a total tether force F_t on the microvillous tethers, and a contact force F_c from the substrate. The sum of the vectors F_t and F_c is equal and opposite to F_s. The cell radius and the lever arm distance D_s are required to relate F_s to F_t and F_c.

tether duration. L_s was determined from the geometry at the contact site (1, 4), using the step distance as the lever arm.

Results

Stepwise Movements in Leukocyte Rolling

To quantitatively study bond dissociation events that underlie the jerky movements of leukocytes during rolling, we developed a computerized imaging system for automated analysis of leukocyte rolling. Previous methods have required manual intervention for each measurement of leukocyte position (1, 11, 24, 56). Our method allows automatic measurement of the position of multiple leukocytes in each video frame, i.e., every 0.033 s. Each cell is automatically tracked from frame to frame. We were therefore able to collect a much larger amount of data and at a higher time resolution than previously possible. Our data are consistent with a contribution of two mechanisms to cell movement during rolling: (a) viscoelastic stretching of tethers (40, 41), i.e., the membranous and microvillous connections between the cell body and the adhesion receptors that are transiently bound to ligand molecules immobilized on the flow chamber wall, and (b) receptor–ligand dissociation events that result in the release, i.e., the dissociation, of the tether (Fig. 2). Tether stretching occurs at a constant velocity that is related to the force on the tether, and gives a smooth movement that should be similar for E-selectin and L-selectin (40). Tether bond dissociation gives jerky movement. Dissociation is faster for L-selectin than for E-selectin (1), and therefore a higher proportion of cell movement during rolling comes from bond dissociation for L-selectin than for E-selectin. This made it possible to obtain the most comprehensive dataset for studies on the kinetics of tether dissociation with L-selectin, which is the central focus of this study. However, datasets obtained with E-selectin are also presented below, and provide support for the general conclusions on L-selectin and some interesting contrasts.

The jerkiness of frame by frame cell movement was visualized and analyzed in several ways. In cell "footprints," pixels were recorded that represent the central portion of

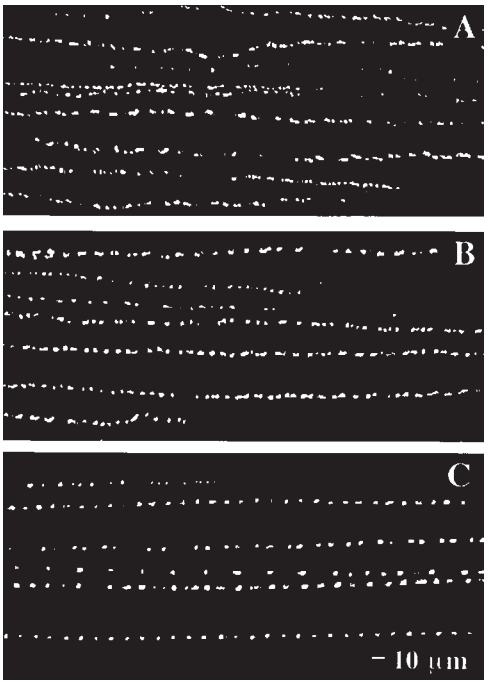

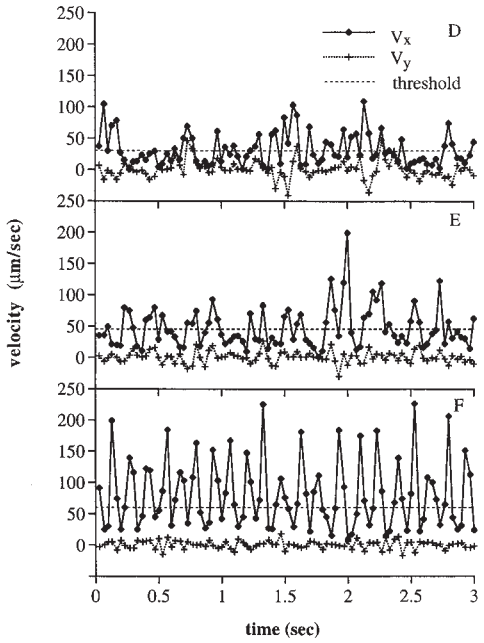

Figure 3. "Footprints" and instantaneous velocities of neutrophils rolling through L-selectin on PNAd. (A–C) Footprints of representative rolling neutrophils on PNAd (1:10) at 2, 8, and 32 dyn/cm^2 of wall shear stress, respectively. Neutrophils rolled with a jerky, step-wise motion. Tightly packed collections of white pixels show the center zone of cells during pauses. (D–F) Instantaneous velocities of representative, individual neutrophils on PNAd (1:10) at 2, 8, and 32 dyn/cm^2 of wall shear stress, respectively. Velocities were determined by measuring the displacement of the cell within successive video frames (0.033 s) in the flow direction (V_x) and in the direction perpendicular to flow (V_y). Dashed line, threshold velocity used in method 1 to define the beginning and end of pauses during rolling.

each cell that showed little or no movement from one video frame to the next (Fig. 3, A–C). Pauses during rolling are thus represented by tightly packed collections of one or more white pixels, and are separated by black spaces over which the cell moved rapidly in "jerks" or "steps." Each cell leaves a trail of footprints that traces the position of its pauses as it rolls across the substrate. At the lowest shear stresses, pauses and steps were evident (Fig. 3 A). However, as the shear stress was raised, the distance between steps became more regular (Fig. 3, B and C), as did the duration of each pause (see below). At higher shears, individualities of cells sometimes became evident. Step distances may be very uniform for individual cells, but differ between cells (data not shown). Rare cells appeared to "limp," taking short steps alternating with long steps (Fig. 3 C, third track from top). Sideways excursions were more pronounced at lower (Fig. 3 A) than higher shear (Fig. 3 C). Sideways movements (V_y in Fig. 3, D–F) correlate with forward movements (V_x in Fig. 3, D–F), and may reflect movement between tethers, at least one of which lies off of a line through the center of the cell in the direction of flow.

In plots of "instantaneous" velocity, the velocity of an individual cell is calculated between each video frame (Fig. 3, D–F). Each stepwise movement is represented by a peak, and each pause by a valley, in the velocity in the direction of flow (V_x, Fig. 3, D–F). At 2 dyn/cm^2, the velocity was ~7.5 μm/s on average in between steps (Fig. 3 D). At 32 dyn/cm^2, regular peaks in velocity representing individual stepwise movements were present, and were separated by valleys in which the velocity was ~36 μm/s on average. The regularity in spacing between the peaks was most marked at 32 dyn/cm^2, showing considerable uniformity in the duration of the pauses between steps. The valleys were similar in height. Often two or three points were present per valley, and the valleys therefore appear to represent a baseline velocity. This baseline velocity appears to reflect the rate of viscoelastic stretching of the tether (Fig. 2, A–C), i.e., the portion of the cell that tethers the cell body to the substrate (40). Peaks separated by valleys of intermediate height were found at intermediate shear stress (Fig. 3 E).

We determined the distribution of step distances during rolling (Fig. 4 A), defining the step distance as the forward travel distance from one velocity peak to the next peak. The 1:20 dilution of PNAd is minimally sufficient to support rolling; at a 1:40 dilution only transient tethers occur (1). At the 1:20 dilution, cells displayed a biphasic distribution of step distances, with the two phases particularly well resolved at low shear, where the modal step distances were 5 and 12 μm, respectively. By comparison, the neutrophil diameter is 8.5 μm. The peak of shorter step distances appears to correspond to steps when one or more receptor–ligand bond is present between the cell and the substrate throughout the step (Fig. 2, A–D). The peak of longer distances appears to correspond to steps during which for the initial part of the step, no bond is present, and new bond formation occurs downstream, similar to a transient tether. The two types of steps may be termed rolling steps and tumbling steps, respectively. A tumbling step can be considered as three successive events (Fig. 2, E–H): (a) a tethering event with a certain number of bonds, (b) an event with zero tether bonds, and (c) a tethering event. Note that if the shear threshold phenomenon is related to the velocity of the cell relative to the substrate, and no bond is present during a tumbling step, as the cell increases in ve-

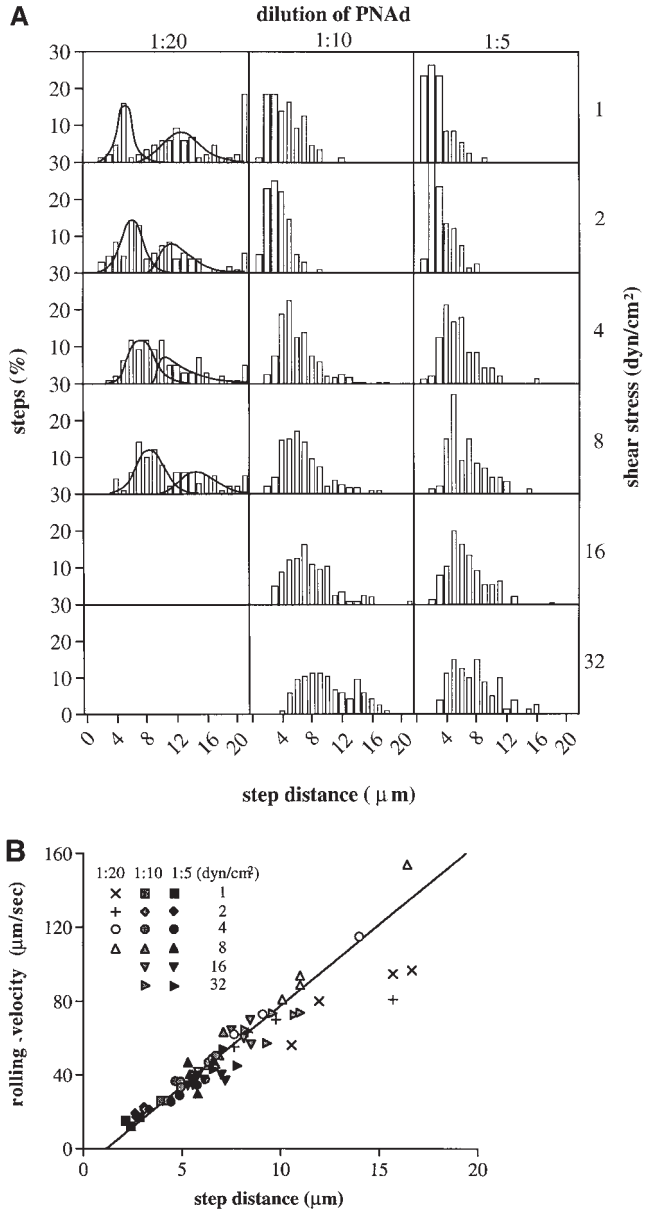

Figure 4. Step distance distribution and its correlation with rolling velocity for neutrophils on PNAd. (A) Step distance distribution. At each indicated shear stress and dilution of PNAd, the step distances in the flow direction were determined using method 2 from the instantaneous velocity of at least three arbitrarily selected rolling cells, >20 steps for each cell. A biphasic distribution of step distances appears at PNAd 1:20 (curved lines) with one phase corresponding to continuous step by step rolling events (rolling steps) and another phase corresponding to tumbling steps. Both types of steps may also be present at 1:10 and 1:5 PNAd, but tumbling steps are less frequent. (B) Rolling velocity as a function of rolling step distance. Each data point presents an average step distance and rolling velocity of an individual rolling cell at the indicated shear stress and dilution of PNAd substrate, determined as in A.

locity the probability of tether formation will increase to a maximum, then decrease with further increase in velocity. This would result in a distribution of tumbling step distances with a well-defined peak, as observed. The presence of a large number of steps of >20 μm at 1:20 PNAd at 1 dyn/cm^2 but not at higher shear is consistent with formation of transient tethers at 1 dyn/cm^2 but not at >2 dyn/cm^2 (1). With increase in shear stress at 1:20 PNAd, the rolling step distance increased, the tumbling step distance decreased or showed little increase, and the proportion of tumbling steps decreased. Thus, average step distance increases with shear. The average rolling step distance of a population of cells is also dependent on the substrate site density. As substrate density increases, step distance decreases (Fig. 4 A). The step distance distributions, and cell footprints (Fig. 3, A–C) show that the tether bonds are intermittantly distributed along the rolling trajectory. Thus when multiple tether bonds are present, the bonds appear to be clustered, and the clusters are separated by a step distance, which ranges on average from 4 (1:20 PNAd) to 2 μm (1:5 PNAd) at low shear (Fig. 4 A).

By contrast to data on cell populations described above, it was of interest that the distribution of rolling step distances for individual cells was much narrower (Fig. 3, B and C). The rolling velocity of individual cells was proportional to step distance, despite differences in PNAd density and wall shear stress (Fig. 4 B). Proportionality between velocity and step distance was maintained for individual cells stably rolling under the same conditions, even though they adopted significantly different rolling velocities and step distances. For example, at 1:10 PNAd and 8 dyn/cm^2, three different cells rolled at (average ±SD) 39.4 ± 5.9, 50.2 ± 13.2, and 63.5 ± 2.0 μm/s, and the same cells had step distances of 5.2 ± 2.3, 6.9 ± 3.0, and 7.2 ± 2.9 μm, respectively.

Kinetic Measurements

Two methods were used here to collect data on the kinetics of tether dissociation during rolling, that gave similar results. (a) A threshold velocity was defined that was ~30 μm/s faster than the baseline velocity due to tether stretching (Fig. 3, D–F, dashed lines). Tether duration was operationally defined as the length of time (number of video frames) spent in the valley at a velocity lower than this threshold. (b) The time for tether dissociation was approximated as the total time per step, i.e., the number of video frames between each rapid decrease and increase in instantaneous velocity. At a dilution of 1:40, PNAd was below the density required to support rolling (Fig. 5 A), and only transient tethers were observed as previously described (1). Although developed for measurements on rolling cells, the first method described above also worked well for measurements on transiently tethered cells on 1:40 PNAd substrates, and yielded transient tether lifetimes of 0.087 ± 0.005 s at 1 dyn/cm^2 and 0.057 ± 0.009 s at 2 dyn/cm^2 (three experiments, average ±SD), in excellent agreement with previous manual measurements (1). Substrates coated at 1:20, 1:10, and 1:5 dilutions of PNAd supported rolling and yielded measurements of rolling tether duration (Fig. 5, B–D). At 1 dyn/cm^2 at all three of these PNAd densities, the tether lifetime for rolling cells was ~0.095 s, almost identical to the lifetime of transient tethers. Furthermore, the rolling tether lifetimes at 1 dyn/cm^2 measured automatically in real time here for large numbers of cells (e.g., 1,100–1,800 tether dissociation measurements

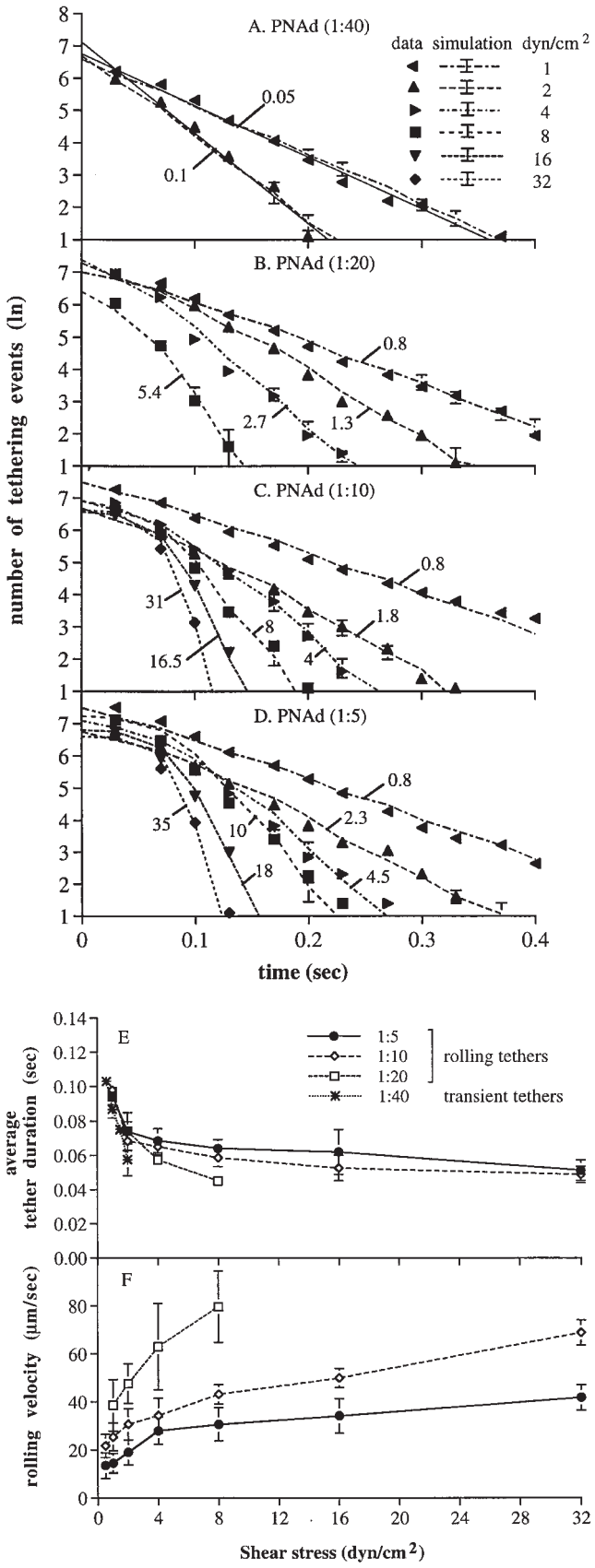

Figure 5. The kinetics of rolling tethers for neutrophils on PNAd. (A–D) Kinetics of dissociation of tethered neutrophils during rolling on PNAd (method 1). Solid symbols, measurements of rolling tether duration for neutrophils at the indicated wall shear stress on the substrate coated with PNAd at 1:40, 1:20, 1:10, and 1:15 dilution, respectively. Dashed lines, Monte Carlo simulations of dissociation of rolling tethers, for a similar number of rolling tethers as measured experimentally. Simulations were initiated with a Poisson distributed number of bonds, giving the average number of bonds shown in the figure; this average number of bonds gave the best fit to the experimental data. (E) Average rolling tether duration as a function of PNAd density and wall shear stress. Average durations were determined from the kinetics of arrest duration measured in A–D. (F) Rolling velocity as a function of PNAd density and wall shear stress. The velocities were determined by measuring the average displacements of rolling neutrophils for 5 s. Bars represent SD of three Monte Carlo simulations; the SD are too small at larger numbers of tethering events and bonds to be visible.

on ~100 rolling cells from three or four different experiments) were in excellent agreement with previous manual measurements from video tape on a necessarily much smaller number of cells (1).

The similarities in lifetimes at 1 dyn/cm^2 for transient tethers and for rolling tethers supports the conclusion that the same quantal unit, which may represent binding and dissociation of a single receptor–ligand bond, is involved in supporting transient tethers and rolling (1). However, at wall shear stresses of 2 dyn/cm^2 and higher, the kinetics of tether dissociation during rolling were not consistent with the presence of a single bond, and suggested that multiple bonds were present. Although the lifetime (average duration) of transient tethers declines exponentially with increasing wall shear stress (Fig. 1), the lifetime of rolling tethers declined much less markedly (Fig. 5 E). Furthermore, at higher wall shear stresses and PNAd density, e.g., (Fig. 5, C and D, 16 and 32 dyn/cm^2), the dissociation kinetics of rolling tethers followed a curved rather than a straight line, consistent with the presence of multiple bonds.

The Model for Dissociation of Clustered Bonds

Therefore, we fit the data on the kinetics of tether dissociation during rolling to a model with multiple bonds. In the model, each individual bond behaves identically to a transient L-selectin tether bond in dissociation kinetics and in influence of applied force on dissociation kinetics. We provided evidence above that the tether bonds are clustered and distributed intermittently along the trajectory of the rolling cell. Of the bonds within the contact zone between the cell and the substrate, our model considers the rearmost cluster of tether bonds that are subjected to tensile force (Fig. 2, A–H). Only these tensed bonds mechanically hold the cell, and thus can be termed the "effective bonds" whose breakage can be detected as a forward jerky movement of the cell. Our model makes no assumptions about whether these effective bonds are on separate microvillous tethers, or on the same microvillous tether (Fig. 2). Our model assumes that each of the effective bonds bears an equal proportion of the total force; e.g., for three bonds, each bears one-third of the total force. When one of these bonds breaks, the force it had borne is distributed equally among the remaining bonds, e.g., the remaining two bonds

*Table I. χ^2 Analysis for Monte Carlo Simulations of the Multiple Bond Model**

Substrate	PNAd (1:40)		PNAd (1:20)				PNAd (1:10)				PNAd (1:5)				E-selectin (200 site μm^{-2})		E-selectin (400 site μm^{-2})	
Method	1		1		2		1		2		1		2		1		1	
Shear stress (dyn cm^{-2})	χ^2	(df)‡	χ^2	(df)	χ^2	(df)	χ^2	(df)	χ^2	(df)	χ^2	(df)	χ^2	(df)	χ^2	(df)	χ^2	(df)
0.5															0.31	(38)	0.21	(38)
1	0.21	(9)	0.08	(10)	0.57	(4)	0.13	(10)	0.17	(6)	0.06	(10)	0.18	(8)	0.53	(32)	0.23	(32)
2	0.24	(4)	0.08	(9)	0.66	(5)	0.06	(7)	0.11	(5)	0.08	(8)	0.003	(6)	0.57	(20)	0.20	(22)
4			0.15	(5)	0.91	(2)	0.02	(5)	0.06	(5)	0.29	(6)	0.10	(6)	0.04	(10)	0.20	(21)
8			0.03	(2)	0.91	(4)	0.07	(3)	0.06	(4)	0.13	(4)	0.25	(5)	0.07	(8)	0.34	(16)
16							0.01	(2)	6.05	(4)	0.03	(2)	2.81	(4)	0.03	(6)		
32							0.01	(2)	1.37	(3)	0.14	(2)	7.42	(3)				

*Data points were compared to Monte Carlo simulations (Fig. 5, A–D, Fig. 7, A–C, and Fig. 10, D and E) and subjected to the χ^2 test (15a). Rolling tether durations and force on the effective tethers were analyzed according to either method 1 or 2.
‡df, Degrees of freedom.

will each bear one-half the total force. The increase in the tensile force on each bond accelerates the dissociation of the remaining effective bonds. The dissociation kinetics of the individual bonds as a function of wall shear stress are assumed to be identical to those previously measured for transient tethers, as confirmed above for rolling at 1 dyn/cm^2, where rolling tethers dissociate with kinetics identical to a single transient tether bond. It is assumed that once tensed bonds break, they do not reform. This is because the selectin, its mucin-like ligand (Fig. 2 I), and the membrane tether to which they are attached (Fig. 2, A–C) will be stretched by the applied force. After unbinding, a return to rest length of the molecules and collapse of the tether from a cylindrical to a spherical shape followed by resorption into the cell (40) will make rebinding unlikely. Stretching and relaxation are particularly expected for the mucin-like ligands of selectins, which at rest have an unstructured backbone and extend ~2 Å/residue (29), and when stressed should easily adopt the extended conformation of the polypeptide chain of 3.8 Å/residue (33). Because the effective bonds are clustered and distributed at the rear edge of the cell, the cell is tethered roughly at the same position (except for tether elongation) until the breakage of all effective bonds, and then moves forward in flow until it is held by the next cluster of tether bonds. The pause duration is the time needed for all the effective bonds to break. For a rolling cell, the number of effective bonds may not be identical in every step, and there appears to be variation between individual cells in the average number of bonds per step. For cell populations, a Poisson distribution gave the best fit to the data over all wall shear stresses; however, for individual cells, bond number may be more narrowly distributed. Theoretic curves for tether dissociation at different shear stresses were estimated by Monte Carlo simulation for different numbers of average bonds per tether (Fig. 5, A–D). Each set of experimental points is plotted with the theoretic curve for the number of bonds that gave the best fit, together with the standard deviations of Monte Carlo simulations for the same number of cells as in the experimental group (Fig. 5, A–D). χ^2 analysis showed that all the fits were consistently good for the model (Table I).

An Increase in Bond Number with Shear

At a PNAd density of 1:40, where only transient tethers occurred, the model curves (dashed) were similar to the straight lines (solid) predicted for first-order dissociation kinetics (Fig. 5 A). Using the model, the best fit to the Poisson distribution was obtained with an average number of bonds per step of 0.05 and 0.1 at 1 and 2 dyn/cm^2, respectively. According to the Poisson distribution, at these shear stresses steps with zero bonds would be present and no tether would be detectable with a frequency of 95 and 90%, respectively, consistent with transient tethers. The remaining events would consist of one, two, or more bonds, with an average of 1.02 and 1.05 bonds per detectable tether at 1 and 2 dyn/cm^2, respectively.

At a low wall shear stress of 1 dyn/cm^2 at 1:20 to 1:5 PNAd, rolling occurs and the model predicts an average of 0.8 bonds per step (Fig. 5, B–D) in agreement with the presence of both rolling steps and tumbling steps. Those tethers that were detectable would contain an average of 1.45 bonds/tether. This is close to 1 bond/tether, and tether dissociation at 1 to 2 dyn/cm^2 followed kinetics that were similar to first order. At 8–32 dyn/cm^2, the rate of dissociation was initially slow, and then accelerated rapidly (Fig. 5, C and D). This nonlinear feature of the dissociation kinetics is characteristic of the multiple bond model, but not a single bond model.

From the fit of the model to the kinetics of tether dissociation during rolling, the number of bonds per tether was estimated as a function of wall shear stress (Fig. 6). The number of tether bonds increased linearly with increasing wall shear stress. There was an intercept at zero wall shear stress that predicts an average of 0.05, 0.08, and 0.27 bonds per tether for PNAd at 1:20, 1:10, and 1:5 dilution, respectively. Thus, as wall shear stress is decreased, the number of bonds per tether will fall to a value too low to support rolling. This is very interesting, because it successfully predicts the finding that rolling through L-selectin requires a wall shear stress above a threshold value, and that the threshold will be found over a range of PNAd densities on the substrate. The slope of the line relating bonds per tether to wall shear stress was dependent on PNAd density (Fig. 6).

Our data suggest that a novel governor mechanism operates to increase the number of bonds per tether as wall shear stress is increased. Such a mechanism is not anticipated by any previous theory of rolling; in fact, it has been anticipated that the number of bonds would decrease

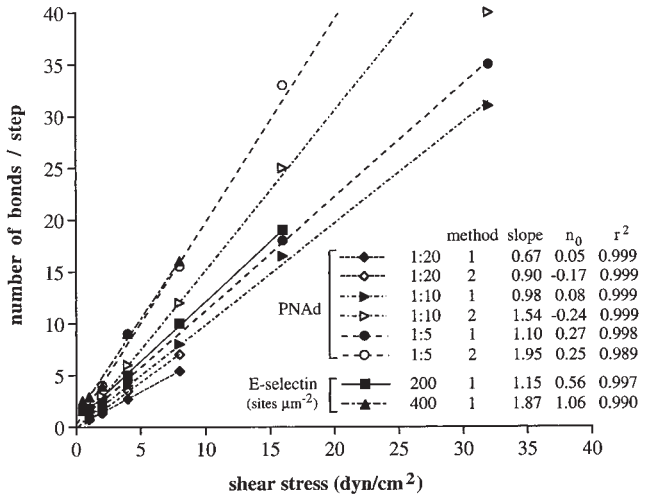

Figure 6. Effect of shear stress on the number of L-selectin–PNAd and E-selectin tether bonds per rolling step. The number of tether bonds per rolling step was estimated from fits to Monte Carlo simulation of dissociation of multiple bonds per step, as shown in Fig. 5, A–D, Fig. 7, A–C, and Fig. 10, D and E. Solid and open symbols, number of bonds estimated by methods 1 and 2, respectively. Slope, increment in bond number with wall shear stress in dyn/cm^2; n_0, intercept of the number of bonds at zero wall shear stress; r^2 is the correlation coefficient for the fit of the data to a straight line.

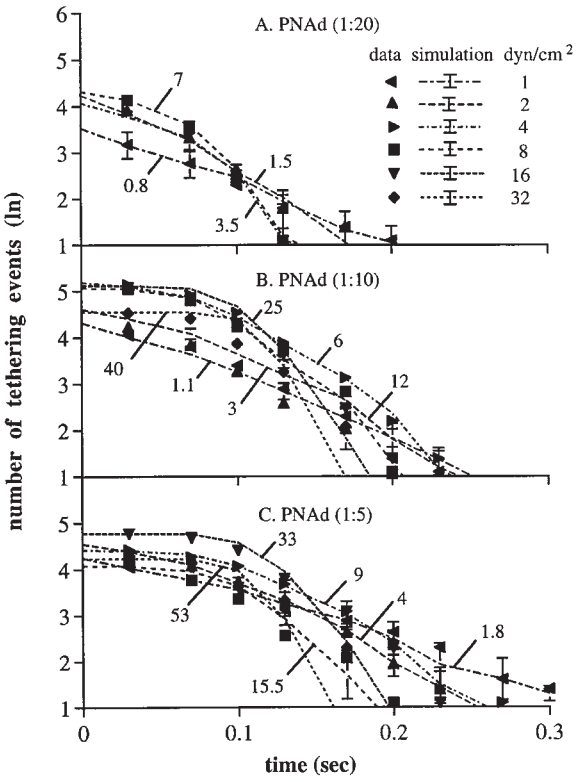

Figure 7. Kinetics of dissociation of tethered neutrophils during rolling on PNAd (method 2). Symbols represent measurements of multiple rolling step durations for each of at least three neutrophils at the indicated wall shear stress and PNAd dilution. The dashed lines and standard deviation bars are for Monte Carlo simulations, that gave the best fit to the data, and estimated the indicated numbers of average bonds per step, as described in the Fig. 5 legend.

rather than increase. The increase in bond number will compensate for the increase in bond off-rate with increasing force, and represents a mechanism to increase the stability of rolling and to make rolling velocity less dependent on the hydrodynamic force on the cell.

The second method for estimating tether duration from the rapid decreases and increases in velocity associated with successive velocity peaks, together with a variable lever arm distance based on the actual observed step distance, was also used to fit the data. The estimated step duration was longer with method 2, yielding estimates of the number of bonds per step that are 1.54 ± 0.17-fold higher. Nonetheless, the fit to the data was good (Fig. 7, A–C, Table I), except at 16 and 32 dyn/cm^2, which may suggest limitations in the model at high shear stresses. Most importantly, method 2 of data analysis also yielded a linear increase in number of bonds with wall shear stress (Fig. 6), and also predicted the shear threshold phenomenon, with ≥1 bond per step below 0.4 and 0.8 dyn/cm^2 at 1:5 and 1:10 PNAd, respectively, close to the observed value of 0.4 to 0.5 dyn/cm^2 (19, 26, 35).

Direct Evidence for an Increase in Bond Number with Shear

The kinetics of rolling tethers suggested that the number of selectin–ligand bonds increased with increasing wall shear stress. To provide further evidence for this, we designed an experiment to directly test the hypothesis that at higher wall shear stresses, more bonds were present between the rolling leukocyte and the substrate. Leukocytes were allowed to roll on PNAd at several different wall shear stresses, and then the wall shear stress was rapidly dropped to 0.3 dyn/cm^2. This value is below the threshold wall shear stress required for rolling, and therefore detachment should occur. We predicted that the higher the wall shear stress before the drop to 0.3 dyn/cm^2, the more the number of bonds, and therefore the longer it should take for the tethers to dissociate. Before the drop in shear, representative cells showed stepwise changes in instantaneous velocity as described above (Fig. 8, A and B). After the drop to 0.3 dyn/cm^2, cells paused, then dissociated from the substrate as shown by movement at the velocity predicted for a cell free in hydrodynamic flow at 0.3 dyn/cm^2. Representative cells that had been rolling at 12 dyn/cm^2 paused longer after the drop to 0.3 dyn/cm^2 (Fig. 8 B) than cells that had been rolling at 2 dyn/cm^2 (Fig. 8 A). The kinetics of cell dissociation from the substrate, defined as the time intervening between the drop to 0.3 dyn/cm^2 and movement at greater than ~30 µm/s, was determined for 41–57 cells at different initial shear stresses (Fig. 8 C). For comparison, rolling tether dissociation kinetics for the same cells before the shear drop, and transient tether dissociation kinetics for cells continuously maintained at 0.3 dyn/cm^2, are shown. The kinetics for dissociation from the substrate after the drop to 0.3 dyn/cm^2 was highly correlated to the velocity at which the cells had been previously

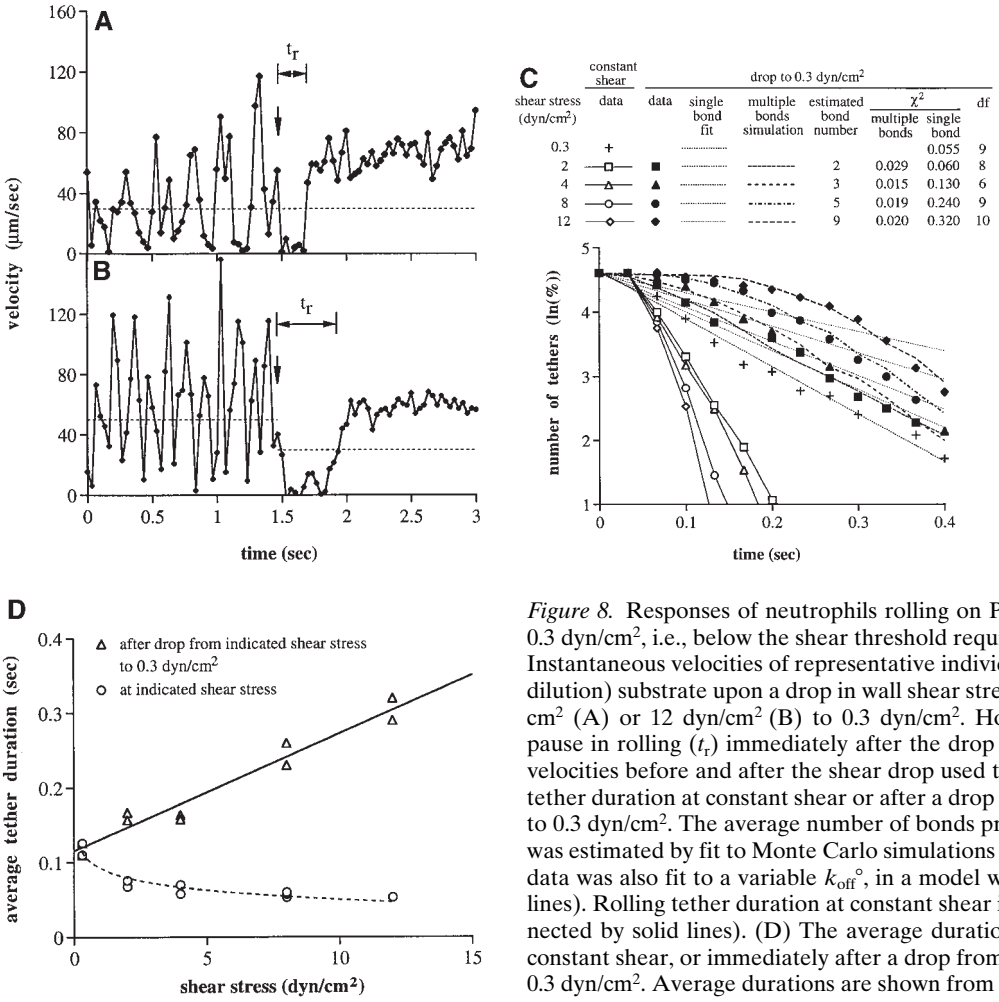

Figure 8. Responses of neutrophils rolling on PNAd to a drop in shear stress to 0.3 dyn/cm^2, i.e., below the shear threshold required to support rolling. (A and B) Instantaneous velocities of representative individual neutrophils on a PNAd (1:10 dilution) substrate upon a drop in wall shear stress (downward arrow) from 2 dyn/cm^2 (A) or 12 dyn/cm^2 (B) to 0.3 dyn/cm^2. Horizontal arrows, duration of the pause in rolling (t_r) immediately after the drop in shear. Dashed lines, threshold velocities before and after the shear drop used to define t_r. (C) Kinetics of rolling tether duration at constant shear or after a drop from the indicated constant shear to 0.3 dyn/cm^2. The average number of bonds present after the reduction in shear was estimated by fit to Monte Carlo simulations (dashed curves). For comparison, data was also fit to a variable k_{off}°, in a model with a single bond (straight dotted lines). Rolling tether duration at constant shear is also shown (open symbols, connected by solid lines). (D) The average duration of rolling tethers, measured at constant shear, or immediately after a drop from the indicated wall shear stress to 0.3 dyn/cm^2. Average durations are shown from two independent experiments.

rolling. After a decrease in shear from 2 dyn/cm^2, the dissociation kinetics were only slightly slower than the transient tether dissociation kinetics for cells continuously maintained at 0.3 dyn/cm^2 (Fig. 8 C). However, as the shear stress at which cells had been rolling increased, there was a marked increase in time required for dissociation, showing that the number of bonds had increased (Fig. 8 D). Furthermore, there was a marked deviation from straight line, first-order dissociation kinetics, with few cells dissociating at early time points (Fig. 8 C).

We compared our model of an increase in the number of receptor–ligand bonds with shear to an alternative model of an increase in affinity of individual bonds, i.e., a decrease in dissociation kinetics accompanied by no change in number of bonds. Dissociation of cells after shift to 0.3 dyn/cm^2 was much slower than for dissociation of rolling tethers (Fig. 8 C), and therefore a larger number of timepoints could be included in statistical comparisons between different models. An F test of χ^2 values showed that the data for dissociation kinetics were better fit by an increase in number of bonds than by a decrease in dissociation kinetics, with P values of 7×10^{-4} to 4×10^{-10} for initial shear stresses of 4–12 dyn/cm^2. The estimated number of bonds to the substrate as a function of wall shear stress ranged from two bonds at 2 dyn/cm^2 to nine bonds at 12 dyn/cm^2. Thus, these results confirmed that the number of bonds between the cell and the substrate increased with increasing wall shear stress.

An Increase in Microvillous Tethers with Shear

An increase with shear in the number of receptor–ligand bonds between the cell and the substrate would also suggest an increase in the number of microvillous tethers between the cell and the substrate. We therefore used an independent method to estimate the number of microvillous tethers. The rate at which individual neutrophil tethers extend, *dl/dt*, has been shown (40, 41) to be related by a constant k_2, to the instantaneous force on the microvillous f_m, over a threshold force F_0: $f_m = F_0 + k_2\, dl/dt$. The initial length (L_0) of 0.35 μm of a microvillus measured by tether pulling (41) agrees well with electron microscopic measurements (10); a tether of this length attached to a round cell body with formation of the next tether bond directly under the body of the cell yields a step distance of 1.75 μm, in excellent agreement with the step distance at low shear (Fig. 4, A and B). The geometric relationship to step distance is used to estimate tether length, L_s. Thus, *dl/dt* is

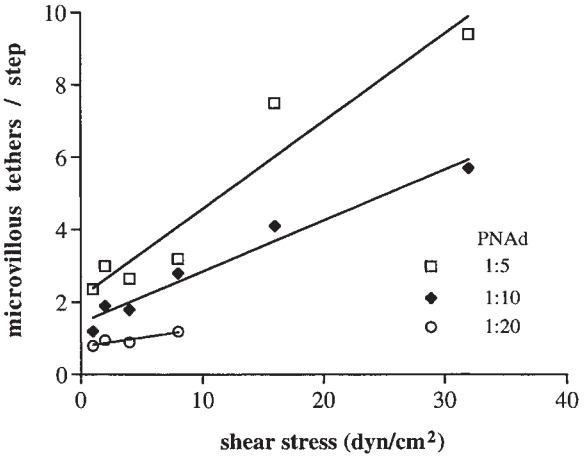

Figure 9. The estimated number of microvillous tethers per step as a function of wall shear stress and PNAd dilution. The average force on a single microvillus can be estimated as: $F_m = F_0 + k_2(L_s - L_0)/T_s$, where F_0 = 45 pN; k_2 = 11 pN*s/μm; L_0, the initial length of a microvillus, = 0.35 μm; L_s is the average tether length; and T_s is the tether duration (41). Assuming that the total tether force, F_t (see Fig. 2 K), is equally distributed over all effectively tethered microvilli, the number of tethered microvilli per step, N_m, was estimated as: $N_m = F_t/F_m$.

estimated as $(L_s - L_0)/T_s$, where T_s is step duration. Then, the average force during tether elongation, $F_m = F_0 + k_2 (L_s - L_0)/T_s$. The total tether force on microvilli, F_t, is estimated as previously described for the force on a tether bond (1, 4, 41). Then, the number of microvillous tethers between the cell and the substrate, N_m, is readily estimated; $N_m = F_t/F_m$ (Fig. 9). At 1:20 PNAd, 0.8–1.2 microvillous tethers per step were estimated from 1 to 8 dyn/cm^2, respectively. A minimum of one microvillous tether per step is required to support rolling, and this is consistent with support of rolling by the 1:20 but not the 1:40 PNAd substrate. At low shear ~1.6 and ~2.7 microvillous tethers per step are estimated at 1:10 and 1:5 PNAd, respectively; at a given shear value, more microvillous tethers were present at higher PNAd densities (Fig. 9). Most importantly, the estimated number of microvillous tethers increased with increasing wall shear stress. Since there must be at least one receptor–ligand bond per microvillous tether, this provides further support for an increase in bond number with wall shear stress.

Stepwise Motion and Kinetics with E-Selectin

To extend results to another selectin, we monitored the rolling of neutrophils on E-selectin. Rolling on E-selectin at 0.5–8 dyn/cm^2 (Fig. 10, A and B) showed jerkiness similar to that on L-selectin, but at higher shear stresses and higher E-selectin densities, rolling became smoother and steps were less well defined (Fig. 10 C). The kinetics of pause duration during rolling on E-selectin were measured over a range of wall shear stresses and at two E-selectin densities (Fig. 10, D and E). The duration of pauses during rolling decreased rapidly from 0.5 to 2 dyn/cm^2, and then tended to a plateau at 4–16 dyn/cm^2. The duration of pauses plateaued at a lower level at 200 than at 400 E-selectin sites/μm^2. These findings are in agreement with the observation that rolling velocity plateaus on E-selectin (27).

The kinetics of rolling tether dissociation on E-selectin were fit to the model of dissociation of multiple selectin–ligand bonds, using previous data on the dissociation kinetics of transient tethers on E-selectin as a function of wall shear stress for the kinetics of dissociation of single E-selectin bonds (1). Fit to the model was good, with χ^2 values and degrees of freedom as shown in Table I. The model predicts that the number of E-selectin bonds increases linearly with increase in shear (Fig. 6).

The increase in number of E-selectin bonds with increase in wall shear stress was confirmed by observations on the effects of a rapid decrease in wall shear stress. When neutrophils rolling at 16 dyn/cm^2 were subjected to a decrease in wall shear stress to 1 dyn/cm^2, the average duration of the next pause was 3.1 s, whereas the average duration of subsequent pauses and of cells rolling continuously at 1 dyn/cm^2 wall shear stress was 0.8 s (a representative cell is shown in Fig. 10 F). Therefore, the number of tether bonds was higher at the higher shear.

It was interesting that after shear reduction, many of the neutrophils rolling on E-selectin moved backwards, i.e., upstream (Fig. 10 F). The representative neutrophil in Fig. 10 F moved back 1.2 μm within 0.4 s. This suggests relaxation, with release of stored energy, of elongated microvillous tethers. Tether stretching appeared to blur rolling steps at high shear, and we were unable to measure pause duration during rolling at 16 dyn/cm^2 or higher on E-selectin at 400 sites/μm^2, and at 32 dyn/cm^2 at 200 sites/μm^2.

Contrasts with Rolling on Antibodies

The motion pattern of rolling on antibodies differed from that on selectins. Leukocytes rolling on antibodies lacked the step-wise movements seen on selectins. There were fluctuations in velocity, but the pattern of motion was smoother over a time scale of seconds. On the other hand, velocity was less stable, because there were fluctuations over a longer time scale of tens of seconds (data not shown). The lack of a stable difference between valleys and peaks in rolling velocity prevented us from measuring pause duration on antibodies. We also attempted to measure pause durations after a reduction in shear from 12 to 5 dyn/cm^2, for JY cells rolling on MEM-124 mAb (14). However, no significantly longer pauses were detected. Therefore, rolling on antibodies appears to lack a regulatory mechanism for increasing bond number with increasing shear.

Discussion

Rolling adhesion has previously been predicted to be an inherently unstable transition state, delicately poised between firm adhesion and lack of adhesion (22). This is emphasized by the failure to observe rolling for many receptor–ligand pairs and for most antibody–surface antigen pairs, even when kinetic rate constants are similar to those for selectins (13, 14, 47, 51). For the small subset of antibody–surface antigen pairs that can mediate rolling, rolling is clearly a transition state phenomenon, with firm adhesion or detachment occurring after small changes in

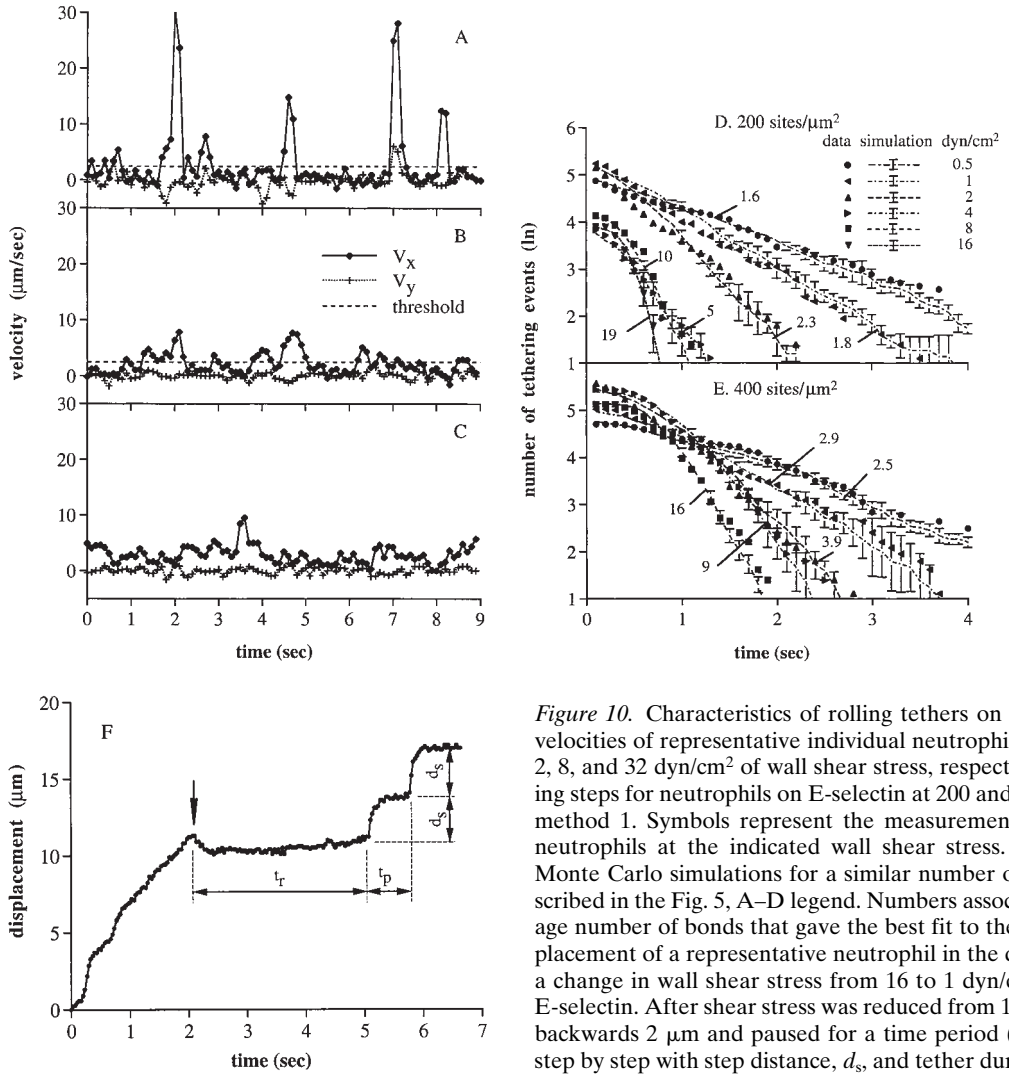

Figure 10. Characteristics of rolling tethers on E-selectin. (A–C) Instantaneous velocities of representative individual neutrophils on E-selectin (200 site/μm^2) at 2, 8, and 32 dyn/cm^2 of wall shear stress, respectively. (D and E) Kinetics of rolling steps for neutrophils on E-selectin at 200 and 400 sites μm^{-2}, determined with method 1. Symbols represent the measurements of rolling tether duration for neutrophils at the indicated wall shear stress. Dashed lines and SD bars are Monte Carlo simulations for a similar number of rolling tether durations, as described in the Fig. 5, A–D legend. Numbers associated with each line are the average number of bonds that gave the best fit to the experimental data. (F) The displacement of a representative neutrophil in the direction of flow before and after a change in wall shear stress from 16 to 1 dyn/cm^2 (arrow), on 200 sites/μm^2 of E-selectin. After shear stress was reduced from 16 to 1 dyn/cm^2 the cell was pulled backwards 2 μm and paused for a time period (t_r) ~3 s and then started rolling step by step with step distance, d_s, and tether duration, t_p, at 1 dyn/cm^2.

antibody density on the substrate or in wall shear stress (14). However, for rolling to function in a robust manner as a mechanism for leukocytes to gauge the level of activating stimuli on endothelium, it must be stable to the large changes in shear that are evident within and between circulatory beds in different tissues, and in exercise and inflammation. We now demonstrate a remarkable biological mechanism for stabilizing rolling that was unanticipated in all previous models of rolling. Previously, the increase in the rate of receptor–ligand dissociation with increase in shear has been predicted, according to the law of mass action, to result in a reduction in the number of receptor–ligand bonds. Opposite to expectation, we find instead an increase in the number of receptor–ligand bonds. Since the rate of bond dissociation is increasing, the counterbalancing mechanism must be an increase in the rate of bond formation with increasing shear. This mechanism not only greatly increases the "parameter space" over which the state of rolling as opposed to firm adhesion or detachment can exist, but also greatly diminishes the impact on rolling velocity of changes in these parameters. The mechanism is analogous to a governor that stabilizes the speed of an engine. An alternative analogy to an automatic braking system is even more apt, as described in detail below.

Multiple lines of evidence support the increase in selectin bond number with shear. Our evidence comes partly from a comparison of the kinetics of tether dissociation during rolling to the kinetics of transient tethers. At low shear, the average lifetime of rolling tethers was consistent with that of transient tethers. However, at higher shear, the average lifetime of rolling tethers was much longer than for transient tethers. Furthermore, at higher shear the rolling tether dissociation curves became non-first order, but fit well to a model of dissociation of multiple receptor–ligand bonds. Good fits were obtained using two different methods for estimating tether duration and the lever arm acting on the tether bonds, although the number of bonds estimated varied 1.5-fold. These estimates may be considered upper and lower limits for the number of tether bonds per rolling step. The fits showed that the number of bonds increased linearly with increase in shear. The increasing uniformity in the time required for tether dissociation with increasing shear on PNAd also supported a multibond model. For a population of cells, the

coefficient of variance for pause lifetime was 96% at 0.3 dyn/cm^2, 47% at 8 dyn/cm^2, and 25% at 32 dyn/cm^2. Pause lifetimes are predicted to become more closely grouped around a mean value as the number of bonds increases, exactly as we find. Direct evidence for an increase in bond number with shear came from a comparison of cells that were rolling at different shear values, and then subjected to a decrease in shear. The average time required for dissociation of the next tether was higher, the higher the shear at which cells had previously been rolling. Furthermore, the dissociation kinetics were decidedly non-first order, and were fit well by a model in which the number of bonds had increased, but not by a model in which the lifetime of a single bond had increased. Again, the fits showed an increase in bond number with increase in shear. The increase in number of L-selectin–PNAd bonds with shear was confirmed and extended with E-selectin–ligand/E-selectin bonds, despite the considerably longer lifetime of the unstressed E-selectin tether bond, a difference in the amount by which off-rate increases in response to hydrodynamic shear force on the cell (1), and possible differences between E-selectin ligands and L-selectin in membrane localization and coupling to the cytoskeleton (18, 53).

Many simplifying assumptions are inherent in our multibond model. These are (a) the tether bonds are clustered and there is an absolute distinction between stressed, effective, and unstressed bonds, (b) applied force is distributed equally over all the effective receptor–ligand bonds, (c) effective bonds do not reassociate after dissociation, (d) the exponential effect of force on the transient tether kinetics can be extrapolated to shear above 2 dyn/cm^2, the limit for measurements on transient tethers, (1, 4), and (e) the number of bonds per rolling step follows a Poisson distribution. There is good justification for each of these assumptions, as explained in the Results. Nonetheless, the situation is obviously more complicated than we have assumed, and our model should be considered a first-order approximation that fits the experimental data, rather than a complete model. The number of bonds per rolling step increased linearly with shear, using two different methods for estimating pause duration from the kinetics of rolling, and a different experimental system for estimating the kinetics of pauses after reduction to low shear. The absolute number of estimated bonds differed between the different systems, but each method gave estimates within 1.5-fold of one of the other methods. We consider this to be excellent agreement, given the differences between the two experimental systems, and methods of estimating tether duration and step distance. The agreement is particularly gratifying because the force per bond is much lower after reduction to low shear, is completely within the range measured for transient tethers, and indeed is so low that there is little effect of force on dissociation kinetics.

The rolling motion of leukocytes in the direction of flow (V_x) contains both step-wise and smooth components. We have provided evidence that each step-wise movement corresponds to dissociation of a cluster of receptor–ligand bonds. Smoother movement certainly includes elongation of microvillous tethers (40, 41) that link the body of the leukocyte to the substrate, but may also include a component from the dissociation of individual receptor–ligand bonds that precede dissociation of the last bond within a cluster. Sideways motion (V_y) also occurred, and was more marked at low wall shear stress, where it correlated with step-wise forward movements. Sideways motion is likely to occur when microvillous tethers form near the edge, rather than near the center, of the adhesive contact zone. Step-wise forward movement would then be accompanied by a sideways movement to center the newly effective bonds with respect to the direction of flow. Note that at higher shear a larger number of microvillous tethers form, and the center of the cluster of microvillous tethers will be on average closer to the center of the adhesive contact zone, and give less sideways motion, as observed.

Under certain conditions, bonds may not be clustered, and this may give rise to apparently smooth movements, as seen for E-selectin at higher shear stresses and substrate densities. Our model may break down when tether elongation accounts for markedly more movement per step than tether dissociation. Indeed, much more tether elongation per step occurs with E-selectin than L-selectin, because of the longer pause duration.

Clear evidence for tether elongation came from observations that cell bodies moved backwards when shear was reduced. At the shears tested, cell bodies did not detectably deform by elongation, and backwards movement clearly reflected tether, not cell body relaxation. Relaxation was much less marked for cells rolling on PNAd than on E-selectin, corresponding to the longer time between steps on E-selectin, which should allow proportionately longer tether elongation. Indeed, almost all cells rolling on E-selectin at 16 dyn/cm^2 moved backwards (0.3–2 μm) when shear was reduced to 1 dyn/cm^2. Elongation of microvillous tethers that link the receptor–ligand bond to the body of the cell enables the cell body to slip relative to the substrate. Microvillous tethers are predicted to be 80 nm in diameter (40), exactly the diameter measured for longer leukocyte microvilli (10). Because of this small diameter, it is reasonable to expect that pulling on receptor–ligand bonds on separate microvilli would elicit separate microvillous tethers, in agreement with our findings of multiple microvillous tethers at higher shear.

Our estimates of the number of microvillous tethers between the cell and the substrate provide independent support for an increase in the number of receptor–ligand bonds with shear, by demonstrating an increase in the number of microvillous tethers between the cell and the substrate. This increase was proportional to wall shear stress, similar to the increase in number of bonds.

Our measurements allow a number of interesting estimates on the nature of the contact zone between the neutrophil and the vessel wall. The equilibrium length of a microvillus is 0.35 μm (10, 41), and both compression and elongation of tethers have been demonstrated. With the reasonable assumptions of tethering of a round cell through a microvillus of this length, the lever arm, i.e., distance between the tether and center of the contact, is 1.75 μm (D_s, Fig. 2 K). This is equal to the unstressed step distance, if it is assumed that formation of the next tether occurs at the center of the contact zone between the cell and the substrate. It is very interesting that the smallest step distances we observed were 2 μm, and that when step distance is extrapolated to zero rolling velocity in Fig. 4 B, the basal value for the step distance with no tether stretch-

ing is estimated to be 1.25 μm, not far from the estimate of 1.75 μm and measurement of 2 μm. Around the circumference of a neutrophil the average distance between microvilli is 0.97 μm (10), and thus the density of microvilli is 1.1/μm^2. A neutrophil 8.5 μm in diameter contains 240 microvilli per cell, and 10 microvilli are present in a contact area 3.5 μm in diameter. This is in agreement with our finding of up to nine microvillous tethers. The contact force F_c (Fig. 2 K) will tend to force and flatten a tethered neutrophil onto the substrate (26); however, the viscosity of the neutrophil cytoplasm is 60,000 times greater than water, and the time scale for deformation is 15–60 s (17, 23, 48). Therefore, in the typical ~0.06 s duration of a L-selectin tether, little flattening will occur. L-selectin is concentrated on the tips of microvilli on neutrophils (10, 34). With ~65,000 L-selectin molecules per cell (38, 42), there are ~260 L-selectin molecules per microvillus. Although at low wall shear stress and PNAd density, only one receptor–ligand bond and microvillous tether appear to be present per step, we estimate a higher number of receptor–ligand bonds per microvillous tether at higher wall shear stresses and PNAd densities. On 1:10 PNAd at 32 dyn/cm^2, we estimate 40 tether bonds and 6.2 microvillous tethers per rolling step. Thus on average, we estimate that approximately seven tether bonds, i.e., seven L-selectin–PNAd bonds, are present at the tip of each microvillous tether under this condition.

We demonstrate that rolling proceeds in steps, which on PNAd at higher shear become remarkably uniform in distance, and uniform in the time required for tether dissociation. This regular pulsatile or oscillatory motion has important consequences for stabilizing the rolling process, and appears to be intimately related to the effective clustering of multiple receptor–ligand bonds to resist force. Oscillatory motion implies a different physical model of rolling than has previously been conceived, and it is important to distinguish it from stochastic motion (22, 24, 56). In stochastic models, step size is a random variable (56). In stochastic motion, there is no tendency or mechanism to obtain regularity in pause duration or step distance; however, we find highly regular step-wise movements during rolling on PNAd at higher shear, both for cell populations and individual cells (Fig. 3, C and F). The importance of regular, oscillatory motion is that it requires an automatic control mechanism to keep motion between certain limits. The tendency of the cell in hydrodynamic flow to increase in velocity must be sensed, and opposed by a mechanism that decreases its velocity. Imagine that the cell in shear flow is analogous to an automobile coasting downhill, with brakes applied to maintain velocity within a certain range. Imagine that the automatic braking system available on late-model automobiles is used. Wheel motion is sensed when brakes are applied, and if wheel motion goes to zero, i.e., the wheel locks, then the brake is released to prevent skidding. On slippery surfaces, the wheels readily lock, and the brakes cycle on and off and cause regular oscillations in velocity, braking force, and wheel motion. This would be analogous to behavior seen under all conditions on PNAd, and at lower site densities and lower wall shear stresses on E-selectin. Under non-slippery conditions, wheels do not lock, brakes are constantly applied, and no oscillations are noted. This would be analogous to behavior seen at higher site densities and higher wall shear stresses on E-selectin. It is a characteristic of automatic control systems that oscillations may occur only under certain conditions (43).

A remarkable feature of our observation of an increase in bonds with wall shear stress is that it shows that the shear threshold phenomenon is not an aberration, but a special case of a general increase in bond number with increase in shear. Below 0.4 dyn/cm^2 on PNAd substrates, transient tethers occur but rolling does not (1). We find that the average number of bonds per step falls below 1 below the threshold; obviously zero bonds will give a lack of adhesion; one or more bonds per step are required to support rolling. A mixture of zero and one bond "events" or "steps" below the shear threshold is consistent with our previous observation of transient tethers under these conditions (1). The shear threshold phenomenon fits well with the use of the Poisson distribution in our model, and with our observation that near the shear threshold on PNAd substrate, there are two populations of step distances that we term rolling steps and tumbling steps. In agreement with the finding that a shear threshold is observed over a wide range of PNAd densities (19), at zero shear the number of bonds extrapolates to 0.05, and 0.08, and 0.27 bonds/step at PNAd densities of 1:20, 1:10, and 1:5, respectively (Fig. 6, method 1). Our data are also in excellent agreement with the finding of a shear threshold for E-selectin, but at a much lower shear than for PNAd–L-selectin, and only at lower E-selectin densities (26). At zero shear the number of bonds on E-selectin extrapolates to 0.56 bonds/step at 200 sites/μm^2, giving a shear threshold, and to 1.06 bonds/step at 400 sites/μm^2, giving no shear threshold (Fig. 6, method 1).

Intuitively, the overall regulation of the rolling process by shear may be extrapolated to the events that occur in each step. We have demonstrated that on average, the number of bonds per step increases with shear. The regular oscillations suggest that during each step, the rate of bond formation is regulated, i.e., undergoes regular, periodic variation. This is exactly as expected for an automatic control system. In order for the automatic control system to give regular oscillations in velocity, the rate of formation of new bonds must be low near the valleys in velocity, and high near the peaks in velocity. This is analogous to what is observed in the shear threshold phenomenon: the rate of bond formation is low at low velocities of the cell relative to the substrate, and higher at higher velocities. We propose a similar change in the rate of bond formation during the cyclical changes in cell velocity relative to the substrate that occur in each step of rolling. It is important to note that this regular variation in the rate of bond formation will give rise to a regular variation in bond density along the trajectory of the rolling cell, and will result in regularly spaced clusters of bonds, exactly as we have observed for the cell footprints during rolling.

The automatic control or feedback system that we propose, here termed an automatic braking system, provides an excellent mechanism for stabilizing rolling velocity to wide variation in substrate site density and wall shear stress. This accords with observations on the stability of the rolling state and rolling velocity in vivo and in vitro. Uniformity in rolling velocity, independent of the varia-

tions in wall shear stress that occur in postcapillary venules within a single tissue, e.g., 3–36 dyn/cm^2 (23a), in different tissues, and in circulatory changes that occur in exercise and inflammation, provides a mechanism to assure relatively uniform exposure to activating stimuli that are important in regulating firm adhesion and diapedesis at inflammatory sites. The increase in rate of bond dissociation with higher shear is compensated by an increase in the rate of bond formation. The overall rate of bond formation is a product of ligand density and the kinetics of bond formation; increase in ligand density is partially compensated by a decrease in kinetics of bond formation.

The data presented here are cellular and kinetic, and do not define the molecular mechanisms underlying the enhancement by shear of bond formation. However, to provide a working hypothesis, and so that readers may have a clearer picture of how an automatic braking system might work at the molecular level, we propose one mechanism that is compatible with current data. We propose that the force or velocity with which selectins contact their ligands is important to overcome or penetrate a repulsive barrier, and promote bond formation. The force or velocity of these molecular contacts would be related to shear and cell velocity relative to the substrate, explaining enhancement of bond formation by shear. We postulate that selectins differ from most other adhesion molecules and from antibodies in requiring velocity or force-dependent mechanisms to promote bond formation. This would explain the instability of rolling on antibodies (14), and our inability to detect regular step-like motions on antibodies.

Mucin-like domains may have an important function in the mechanism for controlling rolling stability. Most selectin ligands are carbohydrate structures present on mucin-like counter-receptors, such as PNAd. By contrast to PNAd, rolling through L-selectin on sialyl Lewis^x glycolipid substrates does not appear to exhibit a shear threshold (19), and is much less stable than rolling on PNAd (2). Furthermore, mild chemical modification of the carbohydrate moieties in PNAd has a marked effect on the shear threshold for L-selectin–dependent rolling (35). Although α4 integrins can support rolling on VCAM-1 (5), which lacks a mucin-like domain, it is interesting that rolling through α4 integrins is more robust on MAdCAM-1, which contains a mucin-like domain (9).

It is fascinating that other known shear-enhanced adhesion mechanisms involve a mucin-like molecule as one of the binding partners. The gpIbα (CD42b, glycocalycin) molecule on platelets mediates shear-enhanced aggregation and rolling of platelets by binding to von Willebrand factor (39). The gpIbα molecule contains a mucin-like domain of 90 residues (30, 54). Shear stimulates flocculation and hence sedimentation of yeast, and a sharp shear threshold is observed (44). The responsible surface glycoprotein, FLO1, is mucin-like (55). Similar to flocculation of yeast, neutrophil L-selectin–dependent aggregation in suspension is also enhanced by shear (45).

Overcoming a repulsive barrier to enable attractive interactions has been discussed previously for aggregation of yeast particles and colloids which is dependent on shear above a threshold (44). Generally, we believe that this is responsible for enhancement of bond formation by shear. Specifically, we speculate that the flexibility of mucin-like domains, which is much greater than that of folded protein domains, is important in shear-enhanced bond formation. When a selectin slowly moves into a space occupied by a mucin-like domain, flexibility will allow a local region of the mucin-like domain to bend out of the way. Furthermore, repulsion by negative charge, and steric repulsion by the mobile glycan groups attached to the mucin, will hinder penetration of the electrostatic and steric "cloud" around the mucin-like domain. More rapid and forceful approach is proposed to promote penetration of this "cloud," and enable contact of the receptor- and ligand-binding sites. A mucin-like domain attached to a receptor-binding domain, as in MAdCAM-1, might also enable the receptor-binding domain to be repelled by the receptor before close contact could be achieved. Work at the molecular level is required to test these hypotheses.

This work was supported by a grant from the National Institutes of Health (HL-48675).

Received for publication 29 October 1998 and accepted without revision.

References

1. Alon, R., S. Chen, K.D. Puri, E.B. Finger, and T.A. Springer. 1997. The kinetics of L-selectin tethers and the mechanics of selectin-mediated rolling. *J. Cell Biol.* 138:1169–1180.
2. Alon, R., T. Feizi, C.-T. Yuen, R.C. Fuhlbrigge, and T.A. Springer. 1995. Glycolipid ligands for selectins support leukocyte tethering and rolling under physiologic flow conditions. *J. Immunol.* 154:5356–5366.
3. Alon, R., R.C. Fuhlbrigge, E.B. Finger, and T.A. Springer. 1996. Interactions through L-selectin between leukocytes and adherent leukocytes nucleate rolling adhesions on selectins and VCAM-1 in shear flow. *J. Cell Biol.* 135:849–865.
4. Alon, R., D.A. Hammer, and T.A. Springer. 1995. Lifetime of the P-selectin: carbohydrate bond and its response to tensile force in hydrodynamic flow. *Nature.* 374:539–542.
5. Alon, R., P.D. Kassner, M.W. Carr, E.B. Finger, M.E. Hemler, and T.A. Springer. 1995. The integrin VLA-4 supports tethering and rolling in flow on VCAM-1. *J. Cell Biol.* 128:1243–1253.
6. Atherton, A., and G.V.R. Born. 1972. Quantitative investigation of the adhesiveness of circulating polymorphonuclear leucocytes to blood vessel walls. *J. Physiol.* 222:447–474.
7. Atherton, A., and G.V.R. Born. 1973. Relationship between the velocity of rolling granulocytes and that of the blood flow in venules. *J. Physiol.* 233: 157–165.
8. Bell, G.I. 1978. Models for the specific adhesion of cells to cells: A theoretical framework for adhesion mediated by reversible bonds between cell surface molecules. *Science.* 200:618–627.
9. Berlin, C., R.F. Bargatze, U.H. von Andrian, M.C. Szabo, S.R. Hasslen, R.D. Nelson, E.L. Berg, S.L. Erlandsen, and E.C. Butcher. 1995. α4 integrins mediate lymphocyte attachment and rolling under physiologic flow. *Cell.* 80:413–422.
10. Bruehl, R.E., T.A. Springer, and D.F. Bainton. 1996. Quantitation of L-selectin distribution on human leukocyte microvilli by immunogold labeling and electron microscopy. *J. Histochem. Cytochem.* 44:835–844.
11. Brunk, D.K., and D.A. Hammer. 1997. Quantifying rolling adhesion with a cell-free assay: E-selectin and its carbohydrate ligands. *Biophys. J.* 72: 2820–2833.
12. Capo, C., F. Garrouste, A-M. Benoliel, P. Bongrand, A. Ryter, and G.I. Bell. 1982. Concanavalin-α-mediated thymocyte agglutination: A model for a quantitative study of cell adhesion. *J. Cell. Sci.* 56:21–48.
13. Chan, P.-Y., M.B. Lawrence, M.L. Dustin, L.M. Ferguson, D.E. Golan, and T.A. Springer. 1991. Influence of receptor lateral mobility on adhesion strengthening between membranes containing LFA-3 and CD2. *J. Cell Biol.* 115:245–255.
14. Chen, S., R. Alon, R.C. Fuhlbrigge, and T.A. Springer. 1997. Rolling and transient tethering of leukocytes on antibodies reveal specializations of selectins. *Proc. Natl. Acad. Sci. USA.* 94:3172–3177.
15. Dembo, M., D.C. Torney, K. Saxman, and D. Hammer. 1988. The reaction-limited kinetics of membrane-to-surface adhesion and detachment. *Proc. R. Soc. Lond.* 234:55–83.
15a. Dowdy, S., and S. Wearden. 1985. Statistics for Research. John Wiley & Sons, New York. 629 pp.
16. Evans, E., and K. Ritchie. 1997. Dynamic strength of molecular adhesion bonds. *Biophys. J.* 72:1541–1555.
17. Evans, E., and A. Yeung. 1989. Apparent viscosity and cortical tension of blood granulocytes determined by micropipet aspiration. *Biophys. J.* 56:

151–160.
18. Finger, E.B., R.E. Bruehl, D.F. Bainton, and T.A. Springer. 1996. A differential role for cell shape in neutrophil tethering and rolling on endothelial selectins under flow. *J. Immunol.* 157:5085–5096.
19. Finger, E.B., K.D. Puri, R. Alon, M.B. Lawrence, U.H. von Andrian, and T.A. Springer. 1996. Adhesion through L-selectin requires a threshold hydrodynamic shear. *Nature.* 379:266–269.
20. Fuhlbrigge, R.C., R. Alon, K.D. Puri, J.B. Lowe, and T.A. Springer. 1996. Sialylated, fucosylated ligands for L-selectin expressed on leukocytes mediate tethering and rolling adhesions in physiologic flow conditions. *J. Cell Biol.* 135:837–848.
21. Graves, B.J., R.L. Crowther, C. Chandran, J.M. Rumberger, S. Li, K.-S. Huang, D.H. Presky, P.C. Familletti, B.A. Wolitzky, and D.K. Burns. 1994. Insight into E-selectin/ligand interaction from the crystal structure and mutagenesis of the lec/EGF domains. *Nature.* 367:532–538.
22. Hammer, D.A., and S.M. Apte. 1992. Simulation of cell rolling and adhesion on surfaces in shear flow: General results and analysis of selectin-mediated neutrophil adhesion. *Biophys. J.* 63:35–57.
23. Hochmuth, R.M., H.P. Ting-Beall, B.B. Beaty, D. Needham, and R. Tran-Son-Tay. 1993. Viscosity of passive human neutrophils undergoing small deformations. *Biophys. J.* 64:1596–1601.
23a. House, S.D., and H.H. Lipowsky. 1987. Leukocyte-endothelium adhesion: microhemodynamics in mesentery of the cat. *Microvasc. Res.* 34:363–379.
24. Kaplanski, G., C. Farnarier, O. Tissot, A. Pierres, A.-M. Benoliel, M.-C. Alessi, S. Kaplanski, and P. Bongrand. 1993. Granulocyte-endothelium initial adhesion: Analysis of transient binding events mediated by E-selectin in a laminar shear flow. *Biophys. J.* 64:1922–1933.
25. Lawrence, M.B., E.L. Berg, E.C. Butcher, and T.A. Springer. 1995. Rolling of lymphocytes and neutrophils on peripheral node addressin and subsequent arrest on ICAM-1 in shear flow. *Eur. J. Immunol.* 25:1025–1031.
26. Lawrence, M.B., G.S. Kansas, E.J. Kunkel, and K. Ley. 1997. Threshold levels of fluid shear promote leukocyte adhesion through selectins (CD62L,P,E). *J. Cell Biol.* 136:717–727.
27. Lawrence, M.B., and T.A. Springer. 1991. Leukocytes roll on a selectin at physiologic flow rates: distinction from and prerequisite for adhesion through integrins. *Cell.* 65:859–873.
28. Lawrence, M.B., and T.A. Springer. 1993. Neutrophils roll on E-selectin. *J. Immunol.* 151:6338–6346.
29. Li, F., H.P. Erickson, J.A. James, K.L. Moore, R.D. Cummings, and R.P. McEver. 1996. Visualization of P-selectin glycoprotein ligand-1 as a highly extended molecule and mapping of protein epitopes for monoclonal antibodies. *J. Biol. Chem.* 271:6342–6348.
30. Lopez, J.A., and J.F. Dong. 1997. Structure and function of the glycoprotein Ib-IX-V complex. *Curr. Opin. Hematol.* 4:323–329.
31. Mehta, P., K.D. Patel, T.M. Laue, H.P. Erickson, and R.P. McEver. 1997. Soluble monomeric P-selectin containing only the lectin and epidermal growth factor domains binds to P-selectin glycoprotein ligand-1 on leukocytes. *Blood.* 90:2381–2389.
32. Nicholson, M.W., A.N. Barclay, M.S. Singer, S.D. Rosen, and P.A. van der Merwe. 1998. Affinity and kinetic analysis of L-selectin (CD62L) binding to GlyCAM-1. *J. Biol. Chem.* 273:763–770.
33. Oberhauser, A.F., P.E. Marszalek, H.P. Erickson, and J.M. Fernandez. 1998. The molecular elasticity of the extracellular matrix protein tenascin. *Nature.* 393:181–185.
34. Picker, L.J., R.A. Warnock, A.R. Burns, C.M. Doerschuk, E.L. Berg, and E.C. Butcher. 1991. The neutrophil selectin LECAM-1 presents carbohydrate ligands to the vascular selectins ELAM-1 and GMP-140. *Cell.* 66: 921–933.
35. Puri, K.D., S. Chen, and T.A. Springer. 1998. Modifying the mechanical property and shear threshold of L-selectin adhesion independently of equilibrium properties. *Nature.* 392:930–933.
36. Puri, K.D., E.B. Finger, G. Gaudernack, and T.A. Springer. 1995. Sialomucin CD34 is the major L-selectin ligand in human tonsil high endothelial venules. *J. Cell Biol.* 131:261–270.
37. Puri, K.D., E.B. Finger, and T.A. Springer. 1997. The faster kinetics of L-selectin than of E-selectin and P-selectin rolling at comparable binding strength. *J. Immunol.* 158:405–413.
38. Rebuck, N., and A. Finn. 1994. Polymorphonuclear granulocyte expression of CD11a/CD18, CD11b/CD18 and L-selectin in normal individuals. *FEMS Immunol. Med. Microbiol.* 8:189–196.
39. Savage, B., E. Saldivar, and Z.M. Ruggeri. 1996. Initiation of platelet adhesion by arrest onto fibrinogen or translocation on von Willebrand factor. *Cell* 84:289–297.
40. Shao, J.-Y., and R.M. Hochmuth. 1996. Micropipette suction for measuring piconewton forces of adhesion and tether formation from neutrophil membranes. *Biophys. J.* 71:2892–2901.
41. Shao, J.-Y., H.P. Ting-Beall, and R.M. Hochmuth. 1998. Static and dynamic lengths of neutrophil microvilli. *Proc. Natl. Acad. Sci. USA.* 95: 6797–6802.
42. Simon, S.I., J.D. Chambers, and L.A. Sklar. 1990. Flow cytometric analysis and modeling of cell-cell adhesive interactions: The neutrophil as a model. *J. Cell Biol.* 111:2747–2756.
43. Stefani, R.T., Jr., C.J. Savant, B. Shahian, and G.H. Hostetter. 1994. Design of feedback control systems. Saunders College Publishing, Orlando, FL. 819 pp.
44. Stratford, M. and P.D.G. Wilson. 1990. Agitation effects on microbial cell-cell interactions. *Lett. Appl. Microbiol.* 11:1–6.
45. Taylor, A.D., S. Neelamegham, J.D. Hellums, C.W. Smith, and S.I. Simon. 1996. Molecular dynamics of the transition from L-selectin-to β_2-integrin-dependent neutrophil adhesion under defined hydrodynamic shear. *Biophys. J.* 71:3488–3500.
46. Tees, D.F.J., and H.L. Goldsmith. 1996. Kinetics and locus of failure of receptor-ligand-mediated adhesion between latex spheres. I. Protein-carbohydrate bond. *Biophys. J.* 71:1102–1114.
47. Tempelman, L.A., and D.A. Hammer. 1994. Receptor-mediated binding of IgE-sensitized rat basophilic leukemia cells to antigen-coated substrates under hydrodynamic flow. *Biophys. J.* 66:1231–1243.
48. Tran-Son-Tay, R., D. Needham, A. Yeung, and R.M. Hochmuth. 1991. Time-dependent recovery of passive neutrophils after large deformation. *Biophys. J.* 60:856–866.
49. Tözeren, A., and K. Ley. 1992. How do selectins mediate leukocyte rolling in venules? *Biophys. J.* 63:700–709.
50. Ushiyama, S., T.M. Laue, K.L. Moore, H.P. Erickson, and R.P. McEver. 1993. Structural and functional characterization of monomeric soluble P-selectin and comparison with membrane P-selectin. *J. Biol. Chem.* 268: 15229–15237.
51. van der Merwe, P.A., A.N. Barclay, D.W. Mason, E.A. Davies, B.P. Morgan, M. Tone, A.K.C. Krishnam, C. Ianelli, and S.J. Davis. 1994. Human cell-adhesion molecule CD2 binds CD58 (LFA-3) with a very low affinity and an extremely fast dissociation rate but does not bind CD48 or CD59. *Biochemistry.* 33:10149–10160.
52. von Andrian, U.H., J.D. Chambers, L.M. McEvoy, R.F. Bargatze, K.E. Arfors, and E.C. Butcher. 1991. Two-step model of leukocyte-endothelial cell interaction in inflammation: distinct roles for LECAM-1 and the leukocyte β_2 integrins *in vivo*. *Proc. Natl. Acad. Sci. USA.* 88:7538–7542.
53. von Andrian, U.H., S.R. Hasslen, R.D. Nelson, S.L. Erlandsen, and E.C. Butcher. 1995. A central role for microvillous receptor presentation in leukocyte adhesion under flow. *Cell.* 82:989–999.
54. Ware, J. 1998. Molecular analyses of the platelet glycoprotein Ib-IX-V receptor. *Thromb. Haemost.* 79:466–478.
55. Watari, J., Y. Takata, M. Ogawa, H. Sahara, S. Koshino, M-L. Onnela, U. Airaksinen, R. Jaatinen, M. Penttila, and S. Keranen. 1994. Molecular cloning and analysis of the yeast flocculation gene *FL01*. *Yeast.* 10:211–225.
56. Zhao, Y., S. Chien, and R. Skalak. 1995. A stochastic model of leukocyte rolling. *Biophys. J.* 69:1309–1320.